[37]C. T. O'Konski and Tae-Kyu Ha, J. Chem. Phys. 49, 5354 (1968).
[38]Values of r_{12} are given in Ref. 1 and by B. P. Stoicheff, Can. J. Phys. 32, 630 (1954). The error quoted here is our own estimate of uncertainty in the value of r_{12} in the solid.
[39]C. J. Jameson and H. S. Gutowsky, J. Chem. Phys. 51, 2790 (1969).
[40]G. Binsch, J. B. Lambert, B. W. Roberts, and J. D. Roberts, J. Am. Chem. Soc. 86, 5564 (1964).
[41]As a purely academic comment we may note that a triplet and a doublet with the observed intensity ratios would also result if d were negligible while $\mathcal{H}_J$ dominated with the condition $J_{\parallel}=J_{\perp}$.
[42]H. Bayer, Z. Physik (Leipzig) 130, 227 (1951).
[43]T. Kushida, J. Sci. Hiroshima Univ. Ser. A 19, 327 (1957).
[44]In order to obtain correct equations it is necessary to symmetrize the rotations about x and y axes because finite rotations do not commute. Equations published in the literature are sometimes in error due to neglect of this fact.
[45]T. Kushida, G. B. Benedek, and N. Bloembergen, Phys. Rev. 104, 1364 (1956).
[46]H. S. Gutowsky and G. A. Williams, Phys. Rev. 105, 464 (1957).
[47]F. D. Murnaghan, Am. J. Math. 59, 235 (1937).
[48]P. M. Mathai and E. J. Allin (private communication).
[49]One must be careful to recognize that averages of the nuclear separation r_{12} over the intramolecular stretching mode are involved that are different in the two cases. The moment of inertia is proportional to $\langle r_{12}^2\rangle$, whereas the dipolar interaction goes as $\langle r_{12}^{-3}\rangle$. The error quoted on the value of r_{12} used encompasses these differences.
[50]J. R. Brookeman, P. C. Canepa, R. Jessup, and T. A. Scott (unpublished).
[51]V. S. Kogan and T. G. Omarov, Zh. Eksperim. i Teor. Fiz. 44, 1873 (1963) [Sov. Phys. JETP 17, 1260 (1963)].
[52]P. G. Klemens, R. DeBruyn Ouboter, and C. le Pair, Physica 30, 1863 (1964).
[53]W. J. Mullin, Phys. Rev. Letters 20, 254 (1968).
[54]J. Duchesne, A. Monfils, and J. Garsou, Physica 22, 816 (1956).
[55]T. Tokuhiro, J. Chem. Phys. 47, 109 (1967).

PHYSICAL REVIEW B VOLUME 4, NUMBER 10 15 NOVEMBER 1971

Theory of the One-Phonon Resonance Raman Effect

Richard M. Martin*
Bell Telephone Laboratories, Murray Hill, New Jersey 07974
(Received 19 March 1971)

Resonant enhancements of Raman scattering cross sections for photons near electronic resonances are calculated for ordinary allowed scattering and for intraband Fröhlich scattering, which is of higher order in the wave vectors and thus forbidden. Exciton effects are included exactly in the hydrogenic approximation via numerical calculations using the Green's-function formulation. Much greater enhancements are found for forbidden than for allowed lines, and it is shown that forbidden lines can become comparable to allowed lines near resonance with large Wannier excitons. It is predicted to be feasible to observe one-LO-phonon lines in crystals (e.g., TlCl and TlBr) in which such transitions are always forbidden. Comparison with experiment for CdS is presented.

I. INTRODUCTION

Large enhancements of Raman scattering cross sections for incident or scattered photons near resonance with fundamental electronic transitions have been observed[1-4] and described theoretically[4-11] in a number of works. The present paper casts in a different form many of the calculations in previous theoretical papers and, in addition, incorporates the electron-phonon intraband Fröhlich interaction.[12] This part of the electron-phonon interaction has been considered previously only by Hamilton[11] for incident light above the band gap. In this paper it is shown to give rise to striking effects in Raman scattering just below the band gap.

All light-scattering processes in which electrons play an important role as intermediate states are expected to exhibit resonance phenomena, with cross sections varying rapidly near allowed electronic resonances, i.e., near peaks in the absorption. Here we are interested in the frequency range just below the lowest absorption edge; the small absorption that is present in real crystals in this range plays no fundamental role and is merely a correction that must be made to experimental data.

Both electron-photon and electron-phonon interactions are here treated in perturbation theory neglecting polariton[8-10,13] and bound-exciton-phonon[14] effects. Thus the present calculations are invalid for photons sufficiently near resonance or for very large exciton-phonon interactions. Expressions for the cross section correctly coupling the exciton and photon into polaritons have been given[8,9] neglecting exciton dispersion, in which case they differ appreciably[9,10] from the perturbation expressions only for $E_{ex}-\omega \leq E_{1t}$, where E_{1t} is the longitudinal-trans-

verse splitting of the exciton. Since in a typical semiconductor E_{1t} is of the order of the intrinsic exciton width ($E_{1t} \sim$ 1 meV in CdS), the perturbation formulas are sufficient except in a very narrow energy range where other broadening effects may also be important. We note, parenthetically, that within the polariton region there may be large corrections to the resonance enhancements given previously[8–10] owing to the wave-vector dependence of the matrix elements described in the present paper.

The intraband Fröhlich interaction scatters the electron and hole from one exciton state to another within the same valence and conduction bands creating or annihilating a phonon that has a macroscopic electric field. [These phonons will be referred to as longitudinal optic (LO), although they need not be strictly longitudinal.] This is the interaction responsible for large LO-phonon-exciton scattering involving phonons of wavelength ~ exciton size as manifested in LO-phonon-assisted absorption,[15] bound-exciton LO sidebands,[16] and the lattice screening in the exciton itself. For any isotropic exciton model, the matrix element for intraband Fröhlich scattering vanishes at long wavelength. Thus, the dominant intraband Fröhlich interaction gives rise to scattering which depends upon the wave vectors of the photons, i.e., is *first-order forbidden* and does not obey the usual selection rules.[17] We shall show that in typical polar semiconductors forbidden LO scattering can, in fact, be large near resonance as has been observed experimentally.[4]

In Sec. II the basic formulas for the Raman cross sections are given incorporating isotropic, but otherwise general, electron-hole correlations, which are essential for intraband Fröhlich scattering. The formulas are valid both above and below the band gap. The actual enhancement factors are calculated in Sec. III, where it is convenient to adopt a Green's-function formulation to treat the internal motion of the electron-hole pair. In this section several results of previous papers are rederived and new results for the intraband Fröhlich scattering are given. In Sec. IV the qualitative dependence of the cross sections upon the relevant crystal parameters is discussed. Comparison with experimental results is given is Sec. V.

II. BASIC FORMULAS

In this section the basic expressions for Raman scattering cross sections are given. The Raman scattering process is viewed (see Fig. 1) as occurring entirely within the crystal and consisting of scattering from an incident photon of frequency ω_i, polarization $\vec{\epsilon}_i$, and wave vector $\vec{k}_i$ to a scattered photon ω_s, $\vec{\epsilon}_s$, $\vec{k}_s$, with the creation of a phonon of type ν, frequency ω_0, and wave vector $\vec{q} = \vec{k}_i - \vec{k}_s$. All wave functions are normalized to the volume of the crystal, V, which is assumed to be large. It is straightforward to relate the cross sections so defined to intensities measured by detectors outside the crystal. The connections are not made explicitly here, but involve only the indices of refraction n for the given rays at ω_i and ω_s. Also, only Stokes scattering at $T = 0$ is considered here; the extension to $T \neq 0$ (anti-Stokes scattering) involves only occupation-number factors (interchange of $\omega_i \rightarrow \omega_s$).[17]

The variation in the index of refraction with incident frequency and between ω_i and ω_s is neglected. This is often a good approximation outside the polariton regions even near the band gap in a semiconductor. Precise measurements[18] of n near the gap in CdS find n considerably larger than $\epsilon_0^{1/2}$ but only a small variation over the region of interest. There are, however, some cases where the variation may be important.

Let W_{fi} be the matrix element for scattering the photon from state i to state s with the creation of the given phonon. Then, from the Golden Rule, the scattering probability per unit solid angle in the scattered beam per unit path length L is

$$S/L = V(n^2\omega_s/2\pi\hbar c^2)^2 |W_{fi}|^2 , \quad (1)$$

where $n = n(\omega_s)$. Thus we can define a Raman cross section per unit cell,

$$\sigma = \Omega(S/L) = \sigma_0 |(m\omega_s n^2/2\pi\hbar e^2)\,\Omega^{1/2} V^{1/2} W_{fi}|^2 , \quad (2)$$

where Ω is the volume of the unit cell and σ_0 is the free-electron Compton cross section

$$\sigma_0 = (e^2/mc^2)^2 . \quad (3)$$

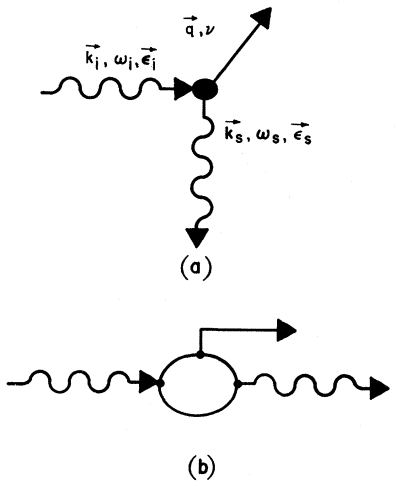

FIG. 1. Raman scattering process. (a) Single scattering of photon from the initial state $\vec{k}_i$, ω_i, $\vec{\epsilon}_i$ to the final (scattered) state $\vec{k}_s$, ω_s, $\vec{\epsilon}_s$ inside the crystal with the creation of a phonon of type ν, wave vector $\vec{q} = \vec{k}_i - \vec{k}_s$. (b) Microscopic diagram of one of six possible orderings of the interactions in Eq. (4) which contribute to (a). This is the only diagram considered in the present work.

The matrix element W_{fi} is a sum of direct photon-phonon and indirect photon-electron-phonon terms. Only the latter are treated here since the former are small for $\omega_i \gg$ lattice frequencies, and indeed are negligible near resonance. The lowest-order indirect contribution to W_{fi} is third order in the interactions,[6,17]

$$W_{fi} = \sum_{\lambda_1,\lambda_2} \frac{\langle 0; s, 1 | H' | \lambda_2 \rangle \langle \lambda_2 | H' | \lambda_1 \rangle \langle \lambda_1 | H' | 0; i, 0 \rangle}{(E_{\lambda_2} - E_{0,i})(E_{\lambda_1} - E_{0,i})} . \tag{4}$$

Here $|0, i, 0\rangle$ denotes the ground electronic state with one photon present in the incident state i and no phonons present, etc., λ_1 and λ_2 run over all possible intermediate states, and H' is the total perturbation

$$H' = H_R + H_L . \tag{5}$$

The electron-photon interaction is[6]

$$H_R = \sum_{\mu} \left(-\frac{e}{m}\right)\left(\frac{2\pi\hbar}{Vn^2\omega_\mu}\right)^{1/2} \vec{\epsilon}_\mu \cdot \vec{p} e^{i\vec{k}_\mu \cdot \vec{r}} a_\mu + \text{c.c.}, \tag{6}$$

where a_μ is a photon destruction operator in state μ. The electron-phonon interaction can be written as one-electron operators

$$H_L = V^{-1/2} \sum_\nu \theta^\nu(\vec{r}) e^{i\vec{q}_\nu \cdot \vec{r}} b_\nu + \text{c.c.}, \tag{7}$$

where ν sums over all phonon modes and wave vectors and $\theta^\nu(r)$ is specified below. There are six possible orderings[17] of the operators in H_R and H_L that contribute to W_{fi}. Here we include only the order shown diagramatically in Fig. 1(b) which often dominates near resonance. (The relative contribution of the other diagrams depends upon many factors and may be important in some cases even near resonance.)

We restrict excited states to those containing a single excited electron, for which the electronic part of the wave function may be written, in the adiabatic approximation,

$$|\lambda, \vec{k}\rangle = \sum_{\substack{c,v \\ \vec{k}}} U_{\lambda\vec{k},cv}(\vec{k}) \Phi_{\vec{k},cv}(\vec{k}), \tag{8}$$

where $\Phi_{\vec{k},cv}(\vec{k})$ is the antisymmetrized product function with one valence Bloch state

$$\Psi_{v,\vec{k}-\vec{\kappa}/2}(\vec{r}) = e^{i(\vec{k}-\vec{\kappa}/2)\cdot\vec{r}} u_{v,\vec{k}-\vec{\kappa}/2}(\vec{r})$$

replaced by a conduction state $\Psi_{c,\vec{k}+\vec{\kappa}/2}$, λ is a composite exciton and band index, and U is the exciton correlation function for the electron and hole. The exciton formalism is convenient, as is shown later, even for the case where the electron-hole correlation is neglected.

All formulas are greatly simplified if we make the isotropic effective-mass approximation and neglect the $\vec{k}$ dependence of the periodic part of the band functions. (The q dependence must be retained to first order, however, for the Fröhlich interaction which has a $1/q$ factor.) Further, we consider only a given set of bands cv, $c'v'$ and assume $m_c^* = m_{c'}^* = m_e^*$ and $m_v^* = m_{v'}^* = m_h^*$. Then dividing λ into band indices cv and an exciton label n, the excitation energies are

$$E_{\lambda,\vec{\kappa}} = E_{cv} + E_n + \hbar^2\kappa^2/[2(m_e^* + m_n^*)] \tag{9}$$

and the correlation function in the center-of-mass coordinate system is[19]

$$\Psi_n(\vec{r}) = e^{-i\alpha\vec{\kappa}\cdot\vec{r}} V^{-1/2} \sum_k U_{n,\vec{\kappa}}(\vec{k}) e^{i\vec{k}\cdot\vec{r}}, \tag{10}$$

which is independent of $\vec{\kappa}$, where $\alpha = \frac{1}{2}(m_e^* - m_h^*)/(m_e^* + m_h^*)$. The excitonic eigenvalues and eigenstates are determined by

$$[-(\hbar^2/2\mu)\nabla^2 + V(r) - E_n]\Psi_n(\vec{r}) = 0, \tag{11}$$

where $\mu^{-1} = m_e^{*-1} + m_h^{*-1}$ is the reciprocal reduced mass and $V(r)$ is the electron-hole interaction potential.

With these approximations the matrix elements of any one-electron operator $f(\vec{r})e^{-i\vec{q}\cdot\vec{r}}$, where $f(\vec{r})$ is periodic and $\vec{q}$ is in the first Brillouin zone (B. Z.), become

$$\langle \lambda'\vec{k}' | f(\vec{r}) e^{-i\vec{q}\cdot\vec{r}} | \lambda\vec{k} \rangle = \delta_{\vec{k},\vec{k}'+\vec{q}} [\delta_{vv'} f_{n'n}(\alpha_e\vec{q}) (u_{c',-\vec{q}/2} | f(r) | u_{c,\vec{q}/2}) - \delta_{cc} f_{n'n}(\alpha_n\vec{q}) (u_{v,-\vec{q}/2} | f(r) | u_{v',\vec{q}/2})], \tag{12}$$

$$\langle \lambda\vec{k} | f(r) e^{-i\vec{q}\cdot\vec{r}} | 0 \rangle = \delta_{0,\vec{k}+\vec{q}} V^{1/2} \Psi_n(\vec{r}=0) (u_{c,-\vec{k}/2} | f(r) | u_{v,\vec{k}/2}). \tag{13}$$

Here ( ) denotes integration over the unit cell,

$$f_{n'n}(\vec{q}) = \int \Psi_{n'}^*(\vec{r}) e^{i\vec{q}\cdot\vec{r}} \Psi_n(\vec{r}) d^3r, \tag{14}$$

$$\alpha_e = -m_h^*/(m_e^* + m_h^*), \quad \alpha_h = m_e^*/(m_e^* + m_h^*). \tag{15}$$

The Raman cross section may now be written out explicitly using (2) and (4) with the definitions (5)–(7) substituted into (12) and (13). All matrix elements are evaluated to *lowest nonzero order* in the wave vectors for each type of interaction. For a phonon of type ν (wave vector $\vec{q}_\nu \equiv q = \vec{k}_i - \vec{k}_s$), we find

$$\sigma_\nu = \sigma_0 \left(\frac{\omega_s}{\omega_i}\right) \left| \sum_{\alpha\beta} \epsilon_s^\alpha R_\nu^{\alpha\beta}(\vec{q}, \omega_i) \epsilon_i^\beta \right|^2, \tag{16}$$

where the Raman tensor is

$$R_\nu^{\alpha\beta}(\vec{q}_j, \omega_i) = \Omega^{1/2} \sum_{\substack{cc' \\ vv'}} \frac{P_{v'c'}^\alpha P_{cv}^\beta}{m} \times [\delta_{vv'} O_{cc'}^\nu(\vec{q}) F_{c'v'cv}(\alpha_e\vec{q}, \omega_i) - \delta_{cc'} O_{vv'}^\nu(\vec{q}) \times F_{c'v'cv}(\alpha_h\vec{q}, \omega_i)] + \cdots . \tag{17}$$

Here, $O_{jj'} = (u_{j,0}|O|u'_{j,0})$ for any operator O and

$$F_{c'v'cv}(\vec{q}, \omega_i) = \sum_{nn'} \frac{\Psi_{n'}(0) f_{n'n}(\vec{q}) \Psi_n(0)}{(E_{c'v'} + E_{n'} - \hbar\omega_i + \hbar\omega_0)(E_{cv} + E_n - \hbar\omega_i)} . \quad (18)$$

(We note that, in general, the exciton functions depend upon the bands through the effective masses.) Since we have taken only the lowest-order terms in $\vec{k}_i$ and $\vec{k}_s$, only s exciton states with $\Psi_n(0) \neq 0$ are involved in the first-order Raman scattering process.

The important properties of the electron-phonon interaction operator $\theta^\nu(\vec{r})$ derive from the spatial range of the interaction. For the deformation-potential (dp)-type interaction,[20] the potential is short range and all wave vectors considered here may be set equal to zero in evaluating the matrix elements. The form $\theta^\nu(\vec{r})$ is then determined solely from crystal symmetry and may be worked out in general.[17] For a two-atom-per-cell crystal,[6,20]

$$\theta^\nu(\vec{r}) = (\hbar\Omega/2ma^2\omega_0)^{1/2} D^\nu(\vec{r}), \quad (19)$$

where D^ν is the dp defined by Bir and Pikus.[20] The Fröhlich interaction, however, is long range and may, in general, be written

$$\theta^\nu = \gamma q^{-1} , \quad (20)$$

where, for a purely longitudinal phonon in a two-atom-per-cell crystal,[6]

$$\gamma = -ie(\epsilon_0^{-1} - \epsilon_s^{-1})^{1/2} (2\pi\hbar\omega_0)^{1/2}, \quad (21)$$

where ϵ_0 is the low-frequency optical dielectric constant and ϵ_s is the static dielectric constant.

To lowest order in the wave vectors for the df, $\theta^\nu_{nn'}$ is just the matrix element of (19). For the Fröhlich interaction, we must expand the Bloch functions to first order in a $\vec{k}\cdot\vec{p}$ series, yielding

$$\theta^\nu_{nn'}(\vec{q}) = \gamma[q^{-1}\delta_{nn'} + \hat{q}\cdot\vec{r}_{nn'}(1 - \Delta_{nn'})] . \quad (22)$$

The first term in (22) is the intraband interaction and the second is interband with the added limitation that $(1 - \Delta_{nn'}) = 0$ if $n = n'$ *or* n and n' are degenerate (e.g., the valence bands neglecting spin-orbit coupling in sphalerite structure crystals). Thus for dp and interband Fröhlich interactions, we find

$$R^{\alpha\beta}_\nu(\vec{q}, \omega_i) \approx \Omega^{1/2} (P^\alpha_{v'c'} P^\beta_{cv}/m) \times (\delta_{cc'}\theta^\nu_{vv'} - \delta_{vv'}\theta^\nu_{cc'}) F_{c'v'cv}(0, \omega_i), \quad (23a)$$

whereas the intraband Fröhlich interaction is determined by the envelope function and

$$R^{\alpha\beta}_\nu(\vec{q}, \omega_i) \approx \Omega^{1/2} \delta_{cc'}\delta_{vv'} (P^\alpha_{vc} P^\beta_{cv}/m) \times \gamma q r_p^2 H_{cv}(\vec{q}, \omega_i), \quad (23b)$$

with

$$H_{cv}(\vec{q}, \omega_i) = (q r_p)^{-2} [F_{cvcv}(\alpha_c\vec{q}, \omega_i) - F_{cvcv}(\alpha_n\vec{q}, \omega_i)], \quad (24)$$

which is independent of q as $q \to 0$. For our purposes a convenient length r_p is the reduced-mass polaron radius $r_p = (2\pi)^{-1}(\hbar/2\mu\omega_0)^{1/2}$.

The Raman tensor for intraband Fröhlich scattering is of higher order in the wave vector, $R^{\alpha\beta}_\nu \propto q$, and hence obeys new selection rules. Because the scattering is intraband, it immediately follows that $R^{\alpha\beta}_\nu$ is large only for $\alpha = \beta$, i.e., only diagonal $(\vec{\epsilon}_i \| \vec{\epsilon}_s)$ scattering is nonvanishing in this order. We shall show that despite being forbidden by the usual selection rules, because of the large characteristic dimensions of the excitonic intermediate states, the cross section may be large near resonance.

III. CALCULATION

The Raman cross section has been given in terms of a sum over all intermediate electronic states denoted by band and exciton labels. Near a resonance the sum over bands is often trivial because the large interband energy differences cause only a small number of bands to be greatly enhanced. It is important, however, to carry out the sum over all exciton states, discrete and continuum, for each set of bands. In this section the sum is carried out for two cases—uncorrelated pairs and Coulomb correlated excitons.

It is convenient to transform the sum into an integral over the Green's functions for the internal motion. Let us define the Green's function for the Schrödinger equation (11),

$$[(-\hbar^2/2\mu)\nabla^2 + V(r) - E] G_E(\vec{r}, \vec{r}') = \delta(\vec{r} - \vec{r}'). \quad (25)$$

It then follows from the relation

$$G_E(\vec{r}, \vec{r}') = \sum_n \frac{\Psi_n(\vec{r}) \Psi^*_n(\vec{r}')}{(E_n - E)} \quad (26)$$

that the needed sum is

$$F_{c'v'cv}(\vec{q}, \omega_i) = \int d^3r\, G_{E_2}(0, \vec{r})\, e^{i\vec{q}\cdot\vec{r}} G_{E_1}(\vec{r}, 0), \quad (27)$$

where

$$E_1 = \hbar\omega_i - E_{cv} - \hbar^2 k_i^2/[2(m_e^* + m_h^*)],$$
$$E_2 = \hbar\omega_i + \hbar\omega_0 - E_{c'v'} - \hbar^2 k_s^2/[2(m_e^* + m_h^*)]. \quad (28)$$

The k_i^2 and k_s^2 terms in (28) are small corrections to the gaps and are neglected here.

The simplest approximation is to neglect all correlations, i.e., set $V(r) = 0$, in which case

$$G_E(\vec{r}, 0) = (2\mu/\hbar^2)(1/4\pi r)\, e^{ikr}, \quad (29)$$

with $k = [(2\mu/\hbar^2)E]^{1/2}$, $\mathrm{Im}k > 0$. Consider only the case where $E_{c'v'} = E_{cv} = E_g$, i.e., scattering between the same or degenerate bands, in which case

TABLE I. Parameters used in calculation of cross sections. Chosen to correspond (approximately) to right-angle scattering in CdS near resonance.

$\epsilon_0 = 5.7$	$m_e^* = 0.2 m_e$
$\epsilon_s = 9.0$	$m_h^* = 1.0 m_e$
$\omega_0 = 37.5$ meV	$a_0 = 54$ a.u.
$\omega_0/E_{1s} = 1.25$	$r_p = 8.5$ a.u.
$n^2 = 8.0$	$qr_p = 0.024$
$p^2/m = 5$ eV	

$$F(q, \omega_i) = \frac{1}{8\pi^2}\left(\frac{\hbar^2}{2\mu}\right)^{-3/2}(\hbar\omega_0)^{-1/2}(qr_p)^{-1} \times \tan^{-1}2\pi q r_p\left[\left(\frac{E_g - \hbar\omega_i}{\hbar\omega_0} - 1\right)^{1/2} - \left(\frac{E_g - \hbar\omega_i}{\hbar\omega_0}\right)^{1/2}\right]. \quad (30)$$

For the dp case, taking $q \to 0$ in Eq. (30) yields the same expression for the Raman tensor as given by Loudon.[17] For the intraband Fröhlich interaction, Eq. (30) is the extension to photons below the band gap of the calculation of Hamilton.[11]

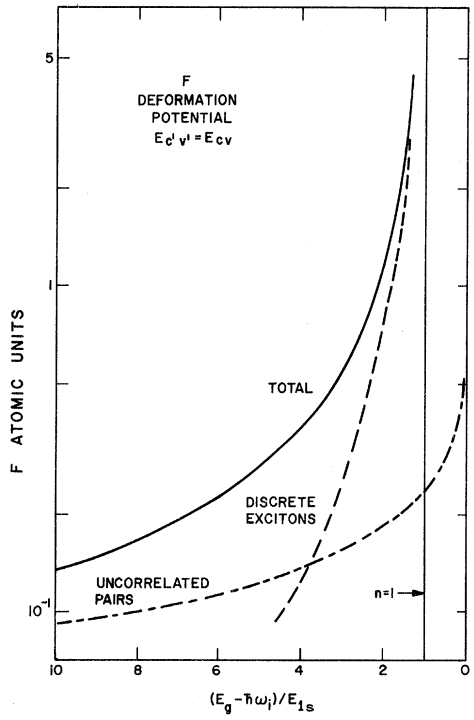

FIG. 2. Scattering amplitude $F(0, \omega_i)$ [see Eqs. (16) and (23a)] for deformation-potential scattering between the same or degenerate bands as a function of $(E_g - \hbar\omega_i)/E_{1s}$, where ω_i is the incident photon frequency, E_g the gap, and E_{1s} the $1s$ exciton binding energy. The parameters in Table I, appropriate for CdS, are used in the calculation. The dot-dashed line is the result if electron-hole correlations are omitted, the dashed line is the result if only discrete excitons are included, and the solid line is the exact result derived from numerical integration of the Green's-function formula (27).

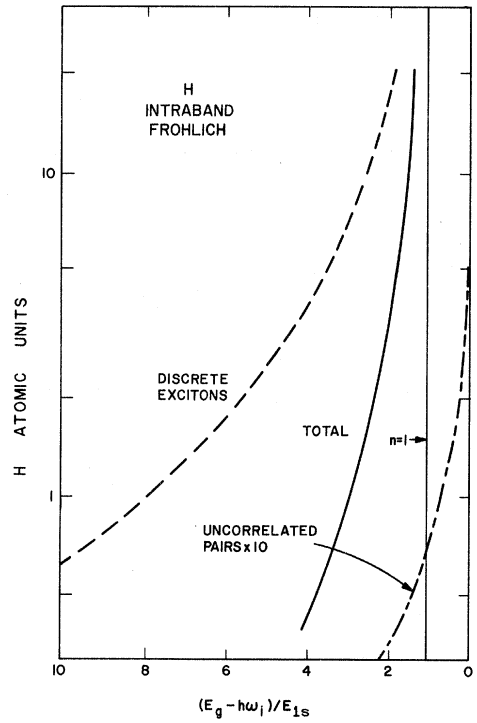

FIG. 3. Scattering amplitude $H(\vec{q}, \omega_i)$ [see Eqs. (16) and (23b)] for intraband Fröhlich scattering. The dot-dashed line is the result if correlations are omitted; dashed line, only discrete excitons; solid line, the exact result of the Green's-function calculation, Eq. (27). See caption of Fig. 2.

Equation (30) has been evaluated using parameters listed in Table I appropriate for right-angle scattering in CdS. The results (in atomic units) for $F = F(0, \omega_i)$ for d.f. and $H = H(q, \omega_i)$ for intraband Fröhlich scattering are given, respectively, in Figs. 2 and 3. [The abscissa is $(E_g - \omega_i)/E_{1s}$, with E_{1s}, the exciton binding energy which is the natural scale to use for comparison with later calculations including exciton effects.] In each case σ approaches a finite value of the band gap.

Coulomb-correlated electron-hole pairs (Wannier excitons) may also be treated straightforwardly. In this case

$$V(r) = e^2/\epsilon r, \quad (31)$$

where ϵ is an appropriate dielectric constant. The Green's function with one coordinate at the origin has a particularly simple form,[21]

$$G_E(\vec{r}, 0) = (2E_{1s})^{-1}a_0^{-3}\Gamma(1-\kappa)(\pi\kappa\rho)^{-1}W_{\kappa,1/2}(\rho), \quad (32)$$

where Γ is the gamma function, W a Whittaker function of the first kind,[22]

$$\kappa = (E_{1s}/E)^{1/2}, \quad \mathrm{Re}\kappa \geq 0, \quad \mathrm{Im}\kappa \geq 0 \tag{33}$$

and

$$\rho = (2/\kappa)(r/a_0),$$

with the Bohr radius and binding energy given by

$$a_0 = \mu/\epsilon, \quad E_{1s} = \tfrac{1}{2}\mu/\epsilon^2 \tag{34}$$

in atomic units, where ϵ is an effective dielectric constant. $G_E(\vec{r}, 0)$ is, of course, isotropic since the Hamiltonian equation (25) is spherically symmetric for $\vec{r}\,' = 0$.

From the formulas of Whittaker and Watson (Ref. 22, p. 340), one can show that for all values of the arguments, a valid representation of W is

$$W_{\kappa,1/2}(\rho) = e^{-1/2\rho}[\Gamma(1-\kappa)]^{-1} U_\kappa(\rho), \tag{35}$$

where

$$U_\kappa(\rho) = \frac{\pi}{\sin\pi\kappa} \sum_{n=0}^{M} A_n(\kappa) \frac{1}{\Gamma(\kappa-n)} (-1)^n \rho^{\kappa-n} + \int_0^\infty dt\, e^{-t}\left[\left(\frac{\rho}{t}+1\right)^\kappa - \sum_{n=0}^{M} A_n(\kappa)\left(\frac{\rho}{t}\right)^{\kappa-n}\right], \tag{36}$$

with

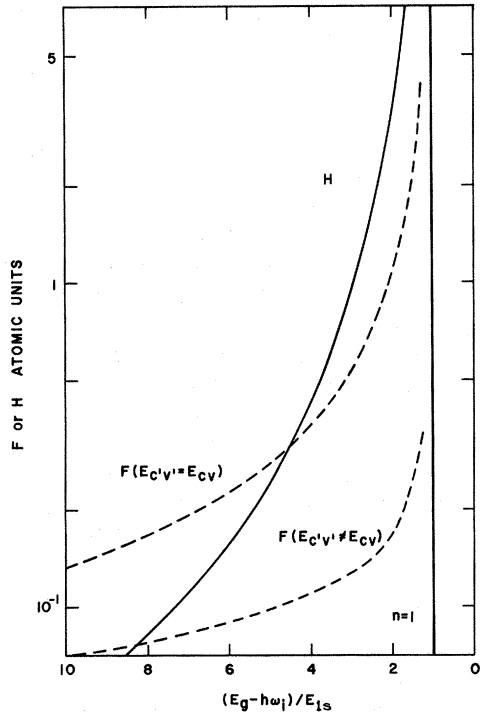

FIG. 4. Comparison of F and H from Figs. 2 and 3. The lower dashed line is the scattering amplitude F for interband deformation or Fröhlich scattering to a band arbitrarily placed $30E_{1s}$ away from the bands at resonance. See caption for Fig. 2.

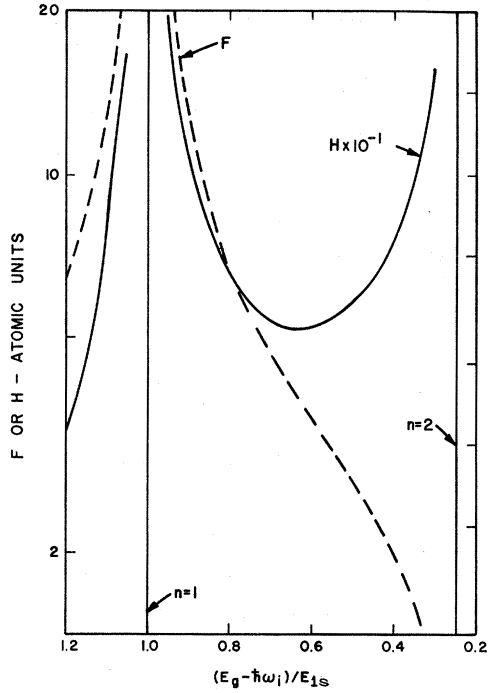

FIG. 5. Comparison of $F(0, \omega_i)$ and $H(\vec{q}, \omega_i)$, respectively, proportional to allowed and forbidden scattering amplitudes, for incident photons between the $n=1$ and $n=2$ exciton resonances. Note that H is very large near the $n=2$ resonance whereas all allowed amplitudes have nodes near $n=2$. The curves have been terminated at fixed distances from the resonances which correspond roughly to the regions where polariton effects and intrinsic broadening become important in CdS. See caption for Fig. 2.

$$A_n(\kappa) = \Gamma(1+\kappa)/[\Gamma(1+\kappa-n)\Gamma(n+1)] \tag{37}$$

and M an integer such that

$$\mathrm{Re}(\kappa-1) < M < \mathrm{Re}\kappa. \tag{38}$$

The integrals in Eq. (27) that involve only the first part of U in (36) can be carried out analytically. The remaining integrals in (27) and (36) are calculated numerically for κ real, i.e., for photon frequencies below the band gap, where the exponential factors make the integrals converge rapidly. The integrals have not been evaluated for photons above the band gap. All resonance divergences are now contained in the Γ functions whose properties are well known. The resulting frequency dependencies of the scattering amplitudes F and H are given as the solid lines in Figs. 2–5. Here also the parameters in Table I were used. Also shown in Figs. 2 and 3 are the results if only discrete excitons are included in the sum over intermediate states. As expected, the total result for F approaches the partial contributions at the appropriate limits. The results for F for dp scattering are the same as those derived by Bendow and Birman.[9]

The scattering amplitude H for the intraband Fröhlich interaction is given in Fig. 3 and compared with F in Figs. 4 and 5. One important result is that for ω_i below all resonances, there is a large cancellation between matrix elements for discrete and continuum states. This greatly decreases the magnitude of H. Far from resonance in all cases the forbidden cross section is, of course, very weak.

The forbidden cross section is a function of scattering geometry, varying as $(\vec{k}_i - \vec{k}_s)^2$ so that σ_F vanishes for forward scattering. Let us note, however, that if the indices of refraction $n(\omega_i)$ and $n(\omega_s)$ are very different (as may be the case, for example, for ω_i above the $1s$ resonance), then $\vec{k}_i - \vec{k}_s$ does not vanish in any geometry.

Figures 4 and 5 clearly show the very different behaviors of the allowed and forbidden scattering amplitudes. The differences arise because of the dependence of the forbidden scattering upon the characteristic lengths of the dominant electronic states and because of differences in the matrix elements between exciton states. Note that the relative magnitudes of the cross sections are not given by Figs. 4 and 5. The relative magnitudes and the dominant features of the enhancement factors are discussed in Sec. IV.

Also shown in Fig. 4 is the enhancement of the scattering amplitude for dp or Fröhlich scattering to a hypothetical band away from resonance with $E_{cv'} - E_{cv}$ arbitrarily chosen to be $30E_{1s}$. Here also only the matrix elements for the diagram in Fig. 1(b) are taken. The resonance is not nearly so sharp as in the case where both intermediate states are near resonance; however, the variation cannot be neglected in any careful analysis of experimental cross sections. In particular, for allowed lines in ZnS-type crystals, the Fröhlich contribution which differentiates LO and TO contains resonance terms *only* of this type. Since LO and TO have very different behavior near resonance it is clear that such terms cannot be omitted.

IV. DISCUSSION

The numerical results for the cross sections including the Coulomb correlations have several features which can be understood from inspection of the Green's function. The most important property of G for the intraband Fröhlich interaction is the spatial extent which is governed by the exponential factor

$$G_E(\vec{r}, 0) \sim e^{-r/(\kappa a_0)} \tag{39}$$

so that there is an energy-dependent effective range $R(E) = (E_{1s}/E)^{1/2} a_0$. It is the variation of the effective range with energy that causes the large variation in the forbidden cross section. In the hydrogenic approximation one finds $R \propto (\mu E)^{-1/2}$, i.e., the range depends only on the reduced mass μ and not on the dielectric constant.

The second important point is that for $\kappa \to$ integer, the function $U_\kappa(\rho)$ in (36) is dominated by the first term in which case the integral over the Green's functions can be done analytically. For example, suppose $\hbar\omega_i \ll |E_{cv}|$ and $|E_{cv} - E_{c'v'}| \ll |E_{cv} - \hbar\omega_i|$, i.e., $\kappa \to 0$. For the dp interaction it is easy to show that

$$\sigma \propto \kappa^2 \propto (E_g - \hbar\omega_i)^{-1} . \tag{40}$$

However, in the same limits for the intraband Fröhlich interaction

$$\sigma \propto \kappa^2 R^4 \propto \kappa^6 \propto (E_g - \hbar\omega_i)^{-3} . \tag{41}$$

Thus the cross section decreases almost as rapidly as if the electronic spectral function were a single spike at E_g [in which case $\sigma \propto (E_g - \hbar\omega_i)^{-4}$]. The asymptotic behavior for both cases (40) and (41) are the same as found neglecting correlations.

The rapid decrease of the forbidden cross section away from resonance agrees with the expectation that Coulomb correlations are important only for states near the band gap; i.e., for a set of states which have only a small fraction of the total oscillator strength. Thus, as anticipated, forbidden cross sections can be large only near resonance.

If the incident photon is between the $1s$ and $2s$ exciton resonances, F and H have very different behavior as is shown in Fig. 5. This is easily understood from Eq. (18). For the dp one has $f_{nn'} = 0$ if $n \neq n'$ and all elements $f_{nn'}$ have the same sign. In this case there must be a null point in the cross section at some frequency between each successive pair of exciton levels so long as $\omega_i - \omega_0 < E_g - E_{1s}$. The analysis is not so simple for the interband Fröhlich interaction, but one can show that the dominant matrix element for $\omega_i \to E_g - E_{1s}$ is opposite in sign to that for $\omega_i \to E_g - E_{ns}$ for $n > 1$. Thus there is no null point for $E_g - E_{1s} < \omega_i < E_g - E_{2s}$. Since the null is found for all allowed scattering processes, the forbidden LO cross section should dominate over all allowed cross sections in this region. The magnitude of the enhancement for $\omega_i \to E_g - E_{2s}$ depends greatly on ω_0; if ω_0 is such that the scattered photon is near resonance with $1s$ ($\omega_0 \approx E_{1s} - E_{2s}$), then H is greatly enhanced, whereas there is no comparable enhancement for allowed scattering.

The relative magnitudes of the cross sections follow from (19) and (21). Consider only cases where $E_{c'v'} = E_{cv}$, i.e., dp (σ_D) and intraband Fröhlich (σ_F) scattering. One finds

$$\sigma_D = A(\Omega/a^2)(m\omega_0^2)^{-1} D^2 |F(0, \omega_i)|^2 \tag{42}$$

and

$$\sigma_F = A\left(\frac{1}{\epsilon_0} - \frac{1}{\epsilon_s}\right) 4\pi e^2 q^2 r_P^4 |H(q, \omega_i)|^2 , \tag{43}$$

with

$$A=\sigma_0\left(\frac{\omega_s}{\omega_i}\right)\hbar\omega_0\Omega\ \frac{P_\alpha^2 P_\beta^2}{2m^2}\ . \tag{44}$$

Therefore, the ratio is

$$\frac{\sigma_F}{\sigma_D}=\frac{4\pi e^2}{\Omega/a^2}\left(\frac{1}{\epsilon_0}-\frac{1}{\epsilon_s}\right)q^2\gamma_P^4 M\omega_{\mathrm{LO}}\omega_{\mathrm{TO}}\,D^{-2}\left|\frac{H}{F}\right|^2\ . \tag{45}$$

For the parameters listed in Table I, (45) becomes (D in eV)

$$\sigma_F/\sigma_D=(0.75/D^2)(H/F)^2. \tag{46}$$

All parameters in σ_F are well known so that the absolute cross section for forbidden one-LO scattering can be predicted. For example, using the parameters in Table I, for $E_g-\omega_i=1.8\times E_{1s}$, we find $\sigma_F=2.3\times10^{-29}$ cm^2/sr or the scattering efficiency $S/L=1.3\times10^{-7}$/cm sr. Other cross sections are easily calculated from Figs. 2–5 and from Eq. (45) if D is known.

The variation of cross section with crystal parameters is readily given. Let us assume E_{1s} is varied but $\omega_0(\gg E_{1s})$ and $(E_g-\omega_i)/E_{1s}$ are held constant. Then in the exciton-dominated region,

$$\sigma_D\propto a_0^{-6}E_{1s}^{-4}E_{1s}\propto\mu^3 \tag{47}$$

and

$$\sigma_F\propto\sigma_D(a_0E_{1s}^{1/2})^4\propto\mu. \tag{48}$$

The additional factor in σ_F includes the fourth-power dependence upon the dominant characteristic length. The same dependence upon μ is found in the regions dominated by nearly uncorrelated intermediate states. The relative cross section, which is the important quantity experimentally, is, therefore, a rapidly varying function of the mass,

$$\sigma_F/\sigma_D\propto\mu^{-2}\ , \tag{49}$$

and is greatly enhanced for small masses.

V. COMPARISON WITH EXPERIMENT

Preliminary measurements of the forbidden LO cross section for three laser frequencies near resonance in CdS at 6 °K have been previously reported[4] along with new measurements of the TO enhancement. The measurements were made in right-angle–scattering geometry denoted $x(zz)y$ with photon polarizations $\vec{\epsilon}_i=\vec{\epsilon}_s=\hat{z}$ along the c axis, $\vec{k}_i=\hat{x}$ and $\vec{k}_s=\hat{y}$. Only the A_1 TO (Γ_1 symmetry) is allowed in this geometry. Near resonance, however, a strong LO line is observed.

Since the photons are polarized along the c axis, only valence bands[23] B and C are strongly resonant. The contribution of the split-off band C, which is 57 meV from B, is important only for the deformation-potential case. In Fig. 6 theoretical and experimental enhancements are compared taking into account the B band only. The experimental points have been corrected for absorption[4] and have estimated errors of ± 25%. It is evident from Fig. 6 that the theoretical and experimental enhancements are in very good agreement.

Only the relative scattering efficiencies or cross sections are considered in Fig. 6; however, absolute cross sections may be determined using the efficiency reported by Arguello, Rousseau, and Porto[24] of $S/L=1.8\times10^{-9}$ cm^{-1}sr^{-1} for A_1 TO at 5145 Å, $x(zz)y$ geometry, and $T=25$ °K (negligible corrections arise from the temperature difference from Ref. 4). Using this value and the relative intensities of Ref. 4 one finds the efficiencies listed in Table II for the forbidden one-LO phonon. For comparison the theoretical values predicted from the parameters in Table I are shown. The agreement is extremely satisfactory since reasonable variations in the parameters lead to roughly a factor of 2 uncertainty in the predicted efficiencies.

The agreement shown for the A_1 TO enhancement must, however, be fortuitous. Ralston *et al.*[3] have recently demonstrated that cancellations occur between different factors in the scattering amplitudes. Therefore, even near resonance the scattering is

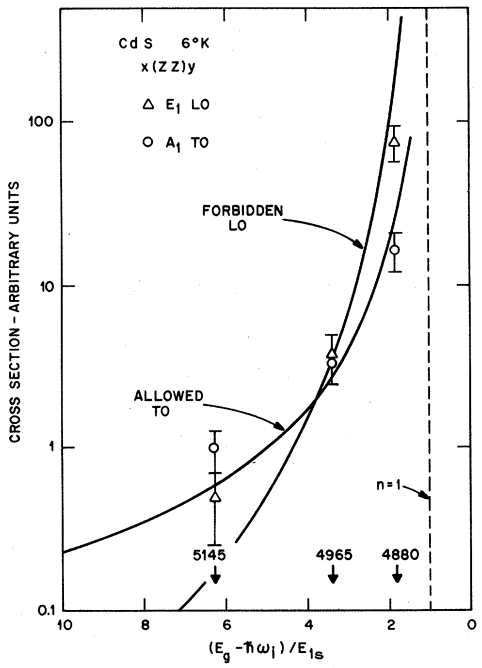

FIG. 6. Comparison with experiment (Ref. 4) for $x(zz)y$ geometry in CdS at three incident photon energies. In this geometry all LO scattering is forbidden. Experimental absorption corrections have been made. Relative LO and TO cross sections are found experimentally and the relative theoretical cross sections have been scaled to fit experiments. Only the B valance band (see Ref. 27) is included in the calculation. The influence of the C band can account for the discrepancy in A_1 TO, but this has not been done here.

TABLE II. Measured and predicted absolute efficiencies of the forbidden one-LO line in CdS. Experimental results are from Ref. 4 and the parameters in Table I were used in the theoretical calculations.

λ (Å)	S/L (10^{-7} cm^{-1} sr^{-1}) Expt.	Theoret.
5145	0.1 ± 0.05	0.1
4965	0.6 ± 0.2	1.3
4880	13 ± 3	28

not dominated by the dp scattering between the top valence bands, and the actual cross section may be quite complicated. The same coments apply for the E_1 TO and allowed LO efficiencies.

It must be emphasized that other mechanisms for forbidden scattering have *not* been conclusively ruled out. Elementary calculations[25] show that impurity-induced extrinsic scattering[25,26] should also occur primarily for $\vec{\epsilon}_i \parallel \vec{\epsilon}_s$ and should be observable with reasonable impurity concentrations. It is therefore appropriate to point out the differences between intrinsic and extrinsic scattering.

In extrinsic scattering momentum is not conserved and the wave vector of the photon q ranges from 0 to roughly the reciprocal of the impurity radius. Thus linewidths should be similar to luminescence one-LO sideband widths.[27] Also there is no dependence upon scattering angle, unlike forbidden intrinsic scattering. Finally resonances should peak at bound-exciton energies.

In the experiment described above and in Ref. 4, the dependence upon scattering angle was *not* checked. The primary evidence[4] in support of the intrinsic mechanism, other than the intensity, is the linewidths which were the same (2.0 ± 0.2 cm^{-1}) as for ordinary allowed scattering.

On the other hand, Colwell and Klein[25] have reported forbidden one-LO scattering from compensated CdS at room temperature. They observed a one-LO line approximately as intense as and broader (30 cm^{-1} vs 20 cm^{-1}) than the two-LO line and showed that the cross section was *independent* of scattering angle. All these results are consistent with impurity-induced scattering and are inconsistent with forbidden intrinsic scattering mechanisms. The contrast between the data of Ref. 25 and that of Ref. 4 show that the difference in samples or temperature may be responsible for very different mechanisms; the cross section measured in Ref. 25 is 2×10^{-4}/cm sr, *two orders of magnitude* greater than that of Ref. 4 extrapolated to comparable energy denominators. The very large cross section of Colwell and Klein[25] also shows that forbidden intrinsic scattering can only be observed under conditions where other mechanisms are suppressed.

VI. CONCLUSIONS

Resonance-enhancement factors for two-phonon Raman scattering cross sections have been calculated for the three types of electron-phonon interactions: deformation potential, interband Fröhlich, and intraband Fröhlich. Coulomb-correlation effects for both discrete and continuum states were included exactly within the isotropic hydrogenic approximation by using the complete Green's function for the hydrogen atom. The enhancement for dp and interband Fröhlich is the same as has been calculated previously.[9,10]

The intraband Fröhlich interaction, however, is treated here for the first time incorporating excitonic effects. Scattering by this mechanism is first-order forbidden, i.e., $\sigma \propto (qR)^2$, where q is the phonon wave vector and R is a characteristic radius of the electronic excitation. Because R can be much larger than typical atomic dimensions for Coulomb-correlated electron-hole pairs near the band gap in a semiconductor, the forbidden scattering can be large near resonance.

The most striking feature of the intraband Fröhlich scattering is that if the excitons are assumed to be isotropic, it contributes only to diagonal $\vec{\epsilon}_i \parallel \vec{\epsilon}_s$ scattering irrespective of the crystal symmetry. Thus one-LO Raman scattering by this mechanism is possible even in crystals in which each atom is at a center of symmetry, when all one-phonon Raman scattering is forbidden by the usual selection rules. TlCl and TlBr are examples of such crystals with large Wannier excitons where forbidden lines should be observable near resonance.

In addition, the dependence of the cross section upon incident-light frequency was shown to be very different for forbidden and allowed lines: The forbidden cross section decreases much more rapidly below resonance and is very large for incident photons between the 1s and 2s resonances, whereas all allowed cross sections pass through null points. The magnitude of the cross section near 2s depends greatly on $\hbar\omega_0/E_{1s}$. The cross section will be greatly enhanced if the scattered photon is near resonance with the 1s exciton, i.e., $\hbar\omega_0 \approx E_{1s} - E_{2s}$. No such enhancement would occur for allowed scattering since the matrix element for $1s \rightarrow 2s$ transitions vanishes.

Finally, as discussed in Refs. 4, 26, and 27, impurity states may also lead to forbidden scattering expected to be largest for one-LO phonons. Contributions from intrinsic and impurity scattering should be experimentally separable through (i) dependence of the cross section on scattering angle, which is isotropic for impurity-induced scattering,

(ii) resonance-enhancement factors, and (iii) line broadening[4,27] in the case of impurity scattering, which is expected to be discernible in an experiment.

ACKNOWLEDGMENTS

The author is indebted to E. O. Kane, T. C. Damen, J. F. Scott, P. J. Colwell, M. V. Klein, and P. Lawaetz for many helpful discussions.

*Present address: Xerox Palo Alto Research Center, 3180 Porter Drive, Palo Alto, Calif. 94304.

[1]J. F. Scott, R. C. C. Leite, and T. C. Damen, Phys. Rev. 188, 1285 (1969), and earlier references given therein.

[2]M. P. Fontana and E. Mullazzi, Phys. Rev. Letters 25, 1102 (1970).

[3]J. M. Ralston, R. L. Wadsack, and R. K. Chang, Phys. Rev. Letters 25, 814 (1970).

[4]R. M. Martin and T. C. Damen, Phys. Rev. Letters 26, 86 (1971).

[5]R. Loudon, J. Phys. (Paris) 26, 677 (1965).

[6]A. K. Ganguly and J. L. Birman, Phys. Rev. 162, 806 (1967).

[7]E. Mulazzi, Phys. Rev. Letters 25, 228 (1970).

[8]D. L. Mills and E. Burstein, Phys. Rev. 188, 1465 (1969).

[9]B. Bendow and J. L. Birman, Phys. Rev. B 1, 1678 (1970); B. Bendow *et al.*, Opt. Commun. 1, 267 (1970).

[10]J. J. Sein, thesis (New York University, 1969) (unpublished).

[11]D. C. Hamilton, Phys. Rev. 188, 1221 (1969).

[12]Y. Toyozawa, Progr. Theoret. Phys. (Kyoto) 20, 53 (1958).

[13]J. J. Hopfield, Phys. Rev. 112, 1555 (1958).

[14]Y. Toyozawa and J. Hermanson, Phys. Rev. Letters 21, 1637 (1968).

[15]B. Segall and G. D. Mahan, Phys. Rev. 171, 935 (1968).

[16]J. J. Hopfield, J. Phys. Chem. Solids 10, 110 (1959).

[17]R. Loudon, Advan. Phys. 13, 423 (1964).

[18]H. Gobrecht and A. Bartschat, Z. Physik 156, 131 (1959).

[19]R. S. Knox, *Theory of Excitons*, Suppl. No. 5 of *Solid State Physics* (Academic, New York, 1963).

[20]G. L. Bir and G. E. Pikus, Fiz. Tverd. Tela. 2, 2287 (1960) [Sov. Phys. Solid State 2, 2039 (1961)].

[21]L. Hostler, J. Math. Phys. 5, 591 (1964); L. Hostler and R. H. Pratt, Phys. Rev. Letters 10, 469 (1963).

[22]F. T. Whittaker and C. N. Watson, *A Course in Modern Analysis* (Cambridge U.P., London, 1963).

[23]D. G. Thomas and J. J. Hopfield, Phys. Rev. 128, 2135 (1962).

[24]C. A. Arguello, D. L. Rousseau, and S. P. S. Porto, Phys. Rev. 191, 1351 (1969).

[25]P. J. Colwell and M. V. Klein, Solid State Commun. 8, 2095 (1970).

[26]M. L. Williams and J. Smit, Solid State Commun. 8, 2009 (1970).

[27]D. C. Reynolds, C. W. Litton, T. C. Collins, and E. N. Frank, *Tenth International Conference on the Physics of Semiconductors*, edited by S. P. Keller, J. C. Hensel, and F. Stern (U.S. AEC, Oak Ridge, Tenn., 1970), p. 519.

PHYSICAL REVIEW B VOLUME 4, NUMBER 10 15 NOVEMBER 1971

Effect of Electronic Polarization on States of Localized Electrons in Insulators*

Shao-fu Wang, Harbans L. Arora, and Mitsuru Matsuura
Department of Physics, University of Waterloo, Waterloo, Ontario, Canada
(Received 11 February 1971)

Starting from the electronic-polaron theory we derive an expression for the interaction between a localized electron and a massive hole via the polarization field for all electron-hole separations. The form of this interaction remains unchanged even when both electron and hole masses are effectively infinite. The expression obtained is compared with the corresponding expression in the Haken-Schottky (HS) theory. Also expressions for polaron effects such as self-energy, mass correction, and Lamb-shift-type corrections are derived in second-order perturbation theory. Owing to the complete analogy between the electron and lattice polarons, our results are also applicable to the case of a bound lattice polaron. Our results are then compared with those of other authors for a bound lattice polaron.

I. INTRODUCTION

From recent work such as those of Refs. 1–3, it is seen that in studying quantum states of a localized electron in insulators, the electronic polarization plays a significant role and considerably affects not only the positions of the electronic energy levels but also the transition energies. In the above references, the treatment of electronic-polarization effects on the system under consideration is based on the electronic-polaron theory of Toyozawa[4] and Haken and Schottky[5] (T-HS). This theory is an analog of the usual lattice-polaron theory and can be used to study not only the effective potential of a source particle but also the polaron effects (such as self-energy, mass correction, and Lamb-